On the Computation of the Complete Spectral Green's Dyadic for Layered Bianisotropic Structures

Francisco Mesa, *Member, IEEE,* Ricardo Marqués, *Member, IEEE,* and Manuel Horno, *Member, IEEE*

***Abstract*— This paper shows how to obtain a systematic algorithm for computing the complete spectral Green's dyadic (CSGD) of multilayered bianisotropic planar structures. The top and bottom boundary conditions of the structures can be either electric/magnetic walls or any kind of boundary condition suitable for implementation by means of impedance/admittance dyadics. The method presented here makes use of the fact that the sheets of normally directed surface electric-/magnetic-current density can be transformed into equivalent sheets of transverse electric-/magnetic-current density. Once the problem has been reduced to deal only with transverse current densities, the equivalent boundary method (EBM) is extended to obtain the CSGD. This method has been applied to compute the radiation characteristics of arbitrarily oriented dipoles embedded in different layered structures.**

***Index Terms*— Arbitrarily oriented dipoles, bianisotropic layered media, dyadic Green's function.**

I. Introduction

THE analysis of the electromagnetic field created by sources or scattered by metallic patches or strips embedded in stratified planar media finds application in many different fields such as geophysical investigations, remote sensing, optoelectronics, microwave circuitry, and antennas. Often, anisotropy is unavoidable in one or more layers of the planar microwave circuits, but in other cases, anisotropic and/or chiral layers are included in planar circuits to improve performance [1], [2]. Magnetic anisotropy can be found in ferrites or may be induced by means of a biasing static magnetic field, thus providing an external parameter to control some characteristics of the circuit and/or the radiation properties of planar antennas [3]–[5]. Also, composite chiral–ferrite media [6] and uniaxial bianisotropic media [7] have been proposed to exploit the electromagnetic properties of these materials. Both the isotropic and all the above cases are particular cases of the most general linear medium, i.e., the bianisotropic medium whose constitutive parameters are dyadics.

The rigorous analysis of planar structures in layered media by the method of moments requires the computation of the dyadic Green's function [8]–[11]. This computation can first be carried out in the spectral domain, where it is possible to obtain closed-form expressions for isotropic structures, and then transforming these to the spatial domain [11]. If anisotropic layers are present, the computation of the spectral Green's dyadic becomes more involved and, in the general bianisotropic case, only a numerical approach can be resorted to. In many problems—e.g., when computing the characteristics of planar circuits—we only need to obtain the *transverse* Green's dyadic, which relates current sources and field components both parallel to the interfaces of the medium (the plane of these interfaces will be termed *transverse*). Numerical procedures for the computation of the transverse spectral Green's dyadic (TSGD) in layered anisotropic media are reported, e.g., in [12]–[15]. Nevertheless, there are also many *planar* structures where the presence of feeding elements breaks the planar condition, making the determination of the complete spectral Green's dyadic (CSGD) unavoidable [16].

One possible way to compute this CSGD is to transform normally directed components of the sources (either electric or magnetic) into equivalent sheets of transverse-surface current density [17]. This procedure enables the application of any of the methods involving only transverse components [12]–[15] to the direct computation of the CSGD. Both the transformations and the general scheme to find the equivalent sources when the sheets of normally directed current are embedded in isotropic media can be found in [17]. In this paper, we will extend this scheme to obtain general expressions for the corresponding transformations when normally directed electric/magnetic currents are embedded in general bianisotropic media.

Once the above transformations are performed, the equivalent boundary method (EBM) [14], [15] may be chosen to compute the CSGD, although other suitable choices are also possible (e.g., [12], [13]). The EBM, proposed by the authors in [14] and [15], is a different approach for systematically computing the TSGD in striplines and/or patches embedded in layered bianisotropic media and provides an straightforward *algorithm* [15] to obtain the transverse components of the electric fields when transverse-surface electric currents are present at some of the interfaces of the layered linear bianisotropic medium. As was discussed in [15], some of the features of the EBM are: 1) the conceptual reduction of the multilayered problem to certain interrelated one-layer problems, 2) the *reduced* size (2×2) of the basic matrices associated with these one-layer problems, which are the elementary blocks of

Manuscript received May 15, 1997; revised November 21, 1997. This work was supported by the CICYT, Spain, under Project TIC95-0447.

The authors are with the Microwave Group, Department of Electronics and Electromagnetism, Facultad de Física, Universidad de Sevilla, 41012 Seville, Spain (e-mail: mesa@cica.es).

Publisher Item Identifier S 0018-9480(98)05503-3.

0018–9480/98$10.00 © 1998 IEEE

the complete algorithm; and 3) the well-conditioned nature of the algorithm, which provides satisfactory numerical behavior for large values of the transverse wave vector (the wave-vector components parallel to the interfaces) and high numbers of layers [18].

Since, to the authors' knowledge, there has not been a method reported to compute the complete electric and magnetic spectral Green's dyadic for layered bianisotropic media, this paper will present a systematic and general scheme to compute the CSGD in bianisotropic media based, first, on the transformation of sheets of normally directed current into equivalent transverse current sheets and, second, on the application of the EBM algorithms. As is well known, obtaining this CSGD is equivalent to calculate the radiation characteristics of an arbitrarily oriented Hertzian dipole [19]. This computation was accomplished in [20] for an isotropic single-layer planar structure via a TE and TM modal decomposition and in [13] and [21] for layered anisotropic structures by a transverse transition matrix method. In this paper, and as an application of our method, we will show some results of the radiation characteristics of arbitrarily oriented Hertzian dipoles embedded in complex layered media.

II. Analysis

The extension of any of the methods proposed in [12]–[15] for the computation of the fields produced by three-dimensional (3-D) sources embedded in a general bianisotropic layered medium creates some difficulties since these methods were originally developed to deal only with transverse-surface electric currents and transverse fields. It should be noted that the latter case is relatively simple because the transverse-surface electric-current densities can be treated as discontinuities of the transverse magnetic fields, and then the problem can be completely solved in terms of just the transverse components. Nevertheless, we can still take advantage of the transverse nature of the above methods by splitting the contribution of the 3-D sources into transverse and normal contributions. Moreover, following a method similar to that reported in [17] for the isotropic case, it will be shown that the normally directed currents embedded in bianisotropic layers can be transformed (in the spectral domain) into equivalent sheets of transverse magnetic- and/or electric-current densities by deriving the field singularities at the location of the dipole sources. In this way, once the transverse fields produced by both the actual and equivalent transverse sources have been obtained, the normal components of the fields can be algebraically computed in terms of the transverse components. The computation of the transverse fields produced by equivalent transverse magnetic sources can be accomplished following the algorithms reported in [12]–[15] for the electric case after applying the duality relationships between electric and magnetic fields [22, pp. 98–100]. The same duality relations can also be used to obtain the fields of original elementary magnetic-current sources. The remainder of this section is organized as follows. Section II-A will show how to obtain the equivalent transverse sources of a 3-D source inside a bianisotropic layer. In Section II-B, the EBM [15] is employed to give the outlines of the systematic computation of the complete Green's dyadic in the spectral domain. Finally, and as an example of application, Section II-C shows how to obtain the spectral Green's dyadic relating the electric field and current in a layered grounded bianisotropic medium.

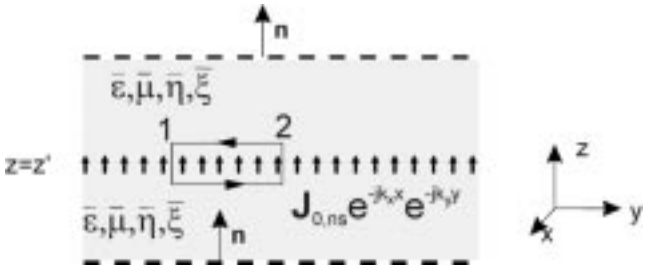

Fig. 1. Sheet of arrayed vertical electric dipoles inside an homogeneous bianisotropic layer.

A. Computation of the Equivalent-Current Sheets

Starting from the method developed in [17, pp. 17–23] for the isotropic case, we will obtain the transverse electric- and/or magnetic-current sheets equivalent to a planar sheet of arrayed vertical electric dipoles inside a general bianisotropic layer (see Fig. 1). Specifically, we will consider a normally directed surface electric-current sheet density given by

$$\mathbf{J}_{ns}(z;\, k_x,\, k_y) = J_{0,\,ns}\delta(z - z')\, e^{-jk_y y}\, e^{-jk_x x}\, e^{j\omega t}\hat{\mathbf{n}} \quad (1)$$

where z' is the z-coordinate of the current sheet, k_x and k_y are the transverse components of the wave vector, and $\hat{\mathbf{n}}$ is the unit vector perpendicular to the interfaces (in the following, the exponentials will be suppressed). This sheet of normally directed current density is placed in a medium characterized by the following bianisotropic and linear constitutive relations [23]:

$$\mathbf{D} = \epsilon_0 \bar{\epsilon}_r \cdot \mathbf{E} + \frac{1}{c}\,\bar{\xi}_r \cdot \mathbf{H} \quad (2)$$

$$\mathbf{B} = \mu_0 \bar{\mu}_r \cdot \mathbf{H} + \frac{1}{c}\,\bar{\eta}_r \cdot \mathbf{E} \quad (3)$$

where $c = 1/\sqrt{\epsilon_0\mu_0}$, $\bar{\epsilon}_r$ and $\bar{\mu}_r$ are the relative dyadic permittivity and permeability, and $\bar{\xi}_r$ and $\bar{\eta}_r$ are the cross-coupling dyadics accounting for the bianisotropy of the substrate.

Following [17], we can consider the surface-density current (1) as the limiting case of a finite sheet of normally directed volume-density current $J_n = J_{0,\,ns}/h$ of thickness h as h approaches zero (see Fig. 2). Owing to the charge-conservation principle, a surface-free charge density given by

$$\pm\rho_s = \frac{J_n}{j\omega} = \frac{J_{0.ns}}{j\omega h} \quad (4)$$

will appear at both bounds of this current sheet.

Since in the limit as h approaches zero some of the fields inside the source region will approach infinity, these fields will determine the field discontinuities across the surface on which the current sheet (1) is placed. Once these predominant fields have been obtained, the sheet of normally directed surface current density will be reduced to an *equivalent* sheet

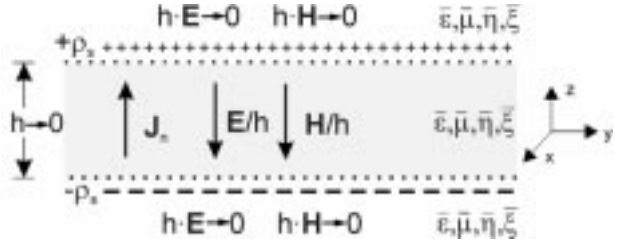

Fig. 2. Finite vertical current sheet inside an homogeneous bianisotropic layer. This sheet turns into the dipole sheet of Fig. 1 as $h \to 0$.

of transverse magnetic and/or electric surface current density giving the same field discontinuities [17, p. 23].

As we are interested only in the behavior of the fields in the source region of the normally directed current sheet in the limit $h \to 0$, these predominant fields are obtained neglecting both variations inside this sheet and the external fields (which should remain finite even in the limit $h \to 0$ [17]). Then, from the continuity conditions at the upper and lower surface charge layers of Fig. 2, it is deduced that inside the source region as $h \to 0$: $h\mathbf{E}_t \to 0$, $h\mathbf{H}_t \to 0$ (subscript t stands for the transverse part of the corresponding vectors) and $h\,B_z \to 0$. In the same way, the z-component of the displacement vector must satisfy $hD_z \to -h\rho_s$, with ρ_s given by (4). Finally, from $h\,B_z \to 0$, $hD_z \to -h\rho_s$ and the constitutive relations (2) and (3), in the limit as h approaches zero, the following equations for E_z and H_z in the bianisotropic case are obtained:

$$\lim_{h\to 0}(-h\rho_s) = \epsilon_{zz} \lim_{h\to 0}(hE_z) + \xi_{zz} \lim_{h\to 0}(hH_z) \tag{5}$$

$$0 = \eta_{zz} \lim_{h\to 0}(h\,E_z) + \mu_{zz} \lim_{h\to 0}(hH_z). \tag{6}$$

These equations, together with (4) and $\lim_{h\to 0}(hJ_n) = J_{0,ns}$, provide the following direct expressions for the dominant fields:

$$\lim_{h\to 0}(hD_z) = -\frac{J_{0,ns}}{j\omega} \tag{7}$$

$$\lim_{h\to 0}(hE_z) = -\frac{1}{j\omega}\,\frac{\mu_{zz}J_{0,ns}}{\epsilon_{zz}\mu_{zz} - \xi_{zz}\eta_{zz}} \tag{8}$$

$$\lim_{h\to 0}(hH_z) = \frac{1}{j\omega}\,\frac{\eta_{zz}J_{0,ns}}{\epsilon_{zz}\mu_{zz} - \xi_{zz}\eta_{zz}} \tag{9}$$

$$\lim_{h\to 0}(h\mathbf{D}_t) = \lim_{h\to 0}(hE_z)(\epsilon_{xz}\hat{\mathbf{x}} + \epsilon_{yz}\hat{\mathbf{y}}) + \lim_{h\to 0}(hH_z)(\xi_{xz}\hat{\mathbf{x}} + \xi_{yz}\hat{\mathbf{y}}) \tag{10}$$

$$\lim_{h\to 0}(h\mathbf{B}_t) = \lim_{h\to 0}(hE_z)(\eta_{xz}\hat{\mathbf{x}} + \eta_{yz}\hat{\mathbf{y}}) + \lim_{h\to 0}(hH_z)(\mu_{xz}\hat{\mathbf{x}} + \mu_{yz}\hat{\mathbf{y}}), \tag{11}$$

where $\hat{\mathbf{x}}$ and $\hat{\mathbf{y}}$ are, respectively, the unit vectors along the x- and y-directions.

If we now proceed along the treatment given in [17, pp. 21–23], starting from

$$\oint \mathbf{E}\cdot d\mathbf{l} = -j\omega \int \mathbf{B}\cdot d\mathbf{S} \tag{12}$$

making use of the integration contour shown in Fig. 1 and taking into account the discontinuity produced in the external (finite) fields of the current sheet shown in Fig. 1 by the infinite fields given in (7)–(11), we obtain

$$\lim_{h\to 0}(hE_{z,2} - hE_{z,1}) + \int_1^2 (\mathbf{E}_t^- - \mathbf{E}_t^+)\cdot d\mathbf{l} = j\omega \int_1^2 \lim_{h\to 0}(h\mathbf{B}_t)(\hat{\mathbf{n}}\times d\mathbf{l}) \tag{13}$$

where $E_{z,2}$ and $E_{z,1}$ are the z-components of the electric fields at positions one and two in Fig. 1 and $\mathbf{E}_t^-$ and $\mathbf{E}_t^+$ the transverse electric fields just above and below the interface $z = z'$. From the above equation, in the limit as points one and two coalesce ($E_{z,2} - E_{z,1} \to dE_z = \nabla_t E_z \cdot d\mathbf{l}$), we can write

$$(\mathbf{E}_t^- - \mathbf{E}_t^+) = \nabla_t \cdot \left[\lim_{h\to 0}(hE_z)\right] + j\omega\hat{\mathbf{n}} \times \lim_{h\to 0}(h\mathbf{B}_t) \tag{14}$$

with ∇_t being the transverse gradient operator. Now taking into account the transverse dependence of the fields [see (1)], (14) can be written as

$$(\mathbf{E}_t^- - \mathbf{E}_t^+) = -j \lim_{h\to 0}(hE_z)\mathbf{k}_t + j\omega\hat{\mathbf{n}} \times \lim_{h\to 0}(h\mathbf{B}_t) \tag{15}$$

where $\mathbf{k}_t = k_x\hat{\mathbf{x}} + k_z\hat{\mathbf{z}}$.

Therefore, the discontinuity produced in $\mathbf{E}_t$ by the sheets of infinite fields (7)–(11) is equivalent to a sheet of surface magnetic-current density $\mathbf{M}_s^{eq}$ given by

$$(\mathbf{E}_t^- - \mathbf{E}_t^+) = \mathbf{M}_s^{eq} \times \hat{\mathbf{n}} \tag{16}$$

$$\mathbf{M}_s^{eq} = -j \lim_{h\to 0}(hE_z)(\mathbf{k}_t \times \hat{\mathbf{n}}) - j\omega \lim_{h\to 0}(h\mathbf{B}_t). \tag{17}$$

Similarly, we find that

$$(\mathbf{H}_t^- - \mathbf{H}_t^+) = \mathbf{J}_s^{eq} \times \hat{\mathbf{n}} \tag{18}$$

where $\mathbf{J}_s^{eq}$ is an equivalent sheet of surface electric-current density given by

$$\mathbf{J}_s^{eq} = -j \lim_{h\to 0}(hH_z)(\mathbf{k}_t \times \hat{\mathbf{n}}) - j\omega \lim_{h\to 0}(h\mathbf{D}_t). \tag{19}$$

Explicit expressions for the above equivalent magnetic and electric currents can be obtained after substituting (8)–(11) into (17) and (19).

From relations (7)–(19), it is apparent that the fields produced by a sheet of arbitrarily directed electric surface current density

$$\mathbf{J}_s(z;\,k_x,\,k_y) = \mathbf{J}_{0,\,s}\delta(z - z')\,e^{-jk_y y}\,e^{-jk_x x} \tag{20}$$

with amplitude $\mathbf{J}_{0,\,s}$ ($\mathbf{J}_{0,\,s} = \mathbf{J}_{0,\,ts} + J_{0,\,ns}\hat{\mathbf{n}}$, with $J_{0,\,ns} = \mathbf{J}_{0,\,s}\cdot\hat{\mathbf{n}}$) are the same than those obtained from the following *equivalent* sheets of surface electric and magnetic currents at $z = z'$:

$$\mathbf{J}_s' = \mathbf{J}_{0,\,ts} + \mathbf{J}_s^{eq} \tag{21}$$

$$\mathbf{M}_s' = \mathbf{M}_s^{eq} \tag{22}$$

where $\mathbf{J}_s^{eq}$ and $\mathbf{M}_s^{eq}$ are given by (17) and (19).

It is interesting to note that for the nonchiral case (when $\overline{\xi} = 0$ and $\overline{\eta} = 0$), the equivalent surface current sheets can

be expressed as

$$\mathbf{J}_s^{eq} = -\frac{\epsilon_{x,z}\hat{\mathbf{x}} + \epsilon_{y,z}\hat{\mathbf{y}}}{\epsilon_{z,z}}\, J_{0,ns} \tag{23}$$

$$\mathbf{M}_s^{eq} = \frac{J_{0,ns}}{\omega\epsilon_{z,z}}\, \mathbf{k}_t \times \hat{\mathbf{n}}. \tag{24}$$

These latter results coincide with those obtained by Tsalamengas [21, eq. (17)] following a quite different method.

The corresponding expressions for the equivalent-surface current sheets of an arbitrarily oriented magnetic source similar to (20) can be obtained from the above equations after applying the duality relations [22, pp. 98–100].

B. Computation of Fields: Outline of the General Procedure

Once the transformation of the original electric-current sheet (20) into equivalent electric and magnetic transverse current sheets has been performed, the fields can be computed following some of the known methods for obtaining the TSGD [12]–[15]. Since the explicit and detailed description of a general algorithm to compute the fields would be rather cumbersome, in this section, we will only give an outline of the general procedure. As was mentioned above, among the possible methods for obtaining the TSGD starting from transverse sources as defined in (21) and (22), the EBM will be used in the following.

Although the direct application of the EBM algorithms in [14] and/or [15] only provides the transverse electric field $\mathbf{E}_t$ produced by the source $\mathbf{J}'_s$ in (21), the $\mathbf{H}_t$ field created by the magnetic source $\mathbf{M}'_s$ (22) can be readily obtained making use of the duality relations [22] together with the corresponding dual-boundary conditions (for instance, electric wall $\leftrightarrow$ magnetic wall and vice versa). If we now were interested in computing the transverse electric field $\mathbf{E}_t$, this can be readily obtained from the values of $\mathbf{H}_t$ at two different levels inside each layer (for example, at the upper and lower interfaces of each layer). Finally, the total electric and/or magnetic field created by both equivalent sources (21) and (22) is obtained by superposition.

After the expressions to compute the transverse fields produced by an electric-current source (20) have been obtained, the duality relations can again be used to obtain the transverse fields produced by a magnetic-current source of a similar type to (20). The remaining E_z and H_z fields can finally be computed from the relations between these z-components and $\mathbf{E}_t$, $\mathbf{H}_t$. These relations are algebraic in the spectral domain and are obtained from (2), (3), and the Maxwell equations in each particular case (explicit expressions for the normally directed fields can be found, for example, in [24]). Obviously, each element of the CSGD can now be obtained as the relation between the corresponding components of fields and sources.

C. Example: Computation of the Transverse Electric Field Created by an Electric-Current Source Inside a Layered Bianisotropic Grounded Medium

As an example, we will explicitly compute the transverse electric field $\mathbf{E}_t$ produced by an arbitrarily oriented electric-current sheet as in (20) embedded in a layered bianisotropic grounded medium as that shown in Fig. 3. We will suppose that the bottom interface of the structure is an electric wall and that the upper interface bounds to free space, although the procedure would work equivalently with other boundary conditions. The source interface ($z = z'$) will be denoted by subscript S (uppercase) and the interface where the fields are to be calculated by subscript F. According to the scheme shown in the above subsection, the transverse field $\mathbf{E}_{t,F}$ can be written as

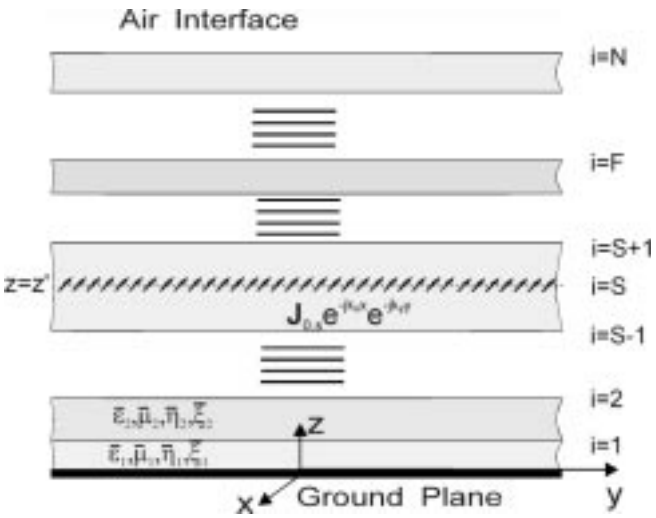

Fig. 3. Arbitrarily oriented phased dipole sheet inside a multilayered bianisotropic grounded structure.

$$\mathbf{E}_{t,F} = \overline{\mathbf{G}}_{EJ} \cdot (\mathbf{J}_{0,ts} + \mathbf{J}_s^{eq}) + \overline{\mathbf{G}}_{EM} \cdot \mathbf{M}_s^{eq} \tag{25}$$

where $\mathbf{J}_{0,ts}$, $\mathbf{J}_s^{eq}$, and $\mathbf{M}_s^{eq}$ are given by (17), (19), and (21), and $\overline{\mathbf{G}}_{EJ}$, $\overline{\mathbf{G}}_{EM}$ are the transverse spectral dyadics relating the transverse electric field to the electric and magnetic sources, respectively.

The transverse Green's dyadic $\overline{\mathbf{G}}_{EJ}$ can be obtained by a direct application of the EBM algorithm, as presented in [15], although, for completeness, an outline of the method for this particular configuration is provided in the Appendix. The computation of the $\overline{\mathbf{G}}_{EM}$ transverse Green's dyadic can be carried out by starting from the transverse electric Green's dyadic of the dual configuration $\overline{\mathbf{G}}_{EJ}^{D}$. This dual configuration results from replacing the lower electric wall by a lower magnetic wall, the free-space impedance by its dual impedance, and each layer constitutive tensors by their duals. The dual electric Green's dyadic actually provides the transverse magnetic field $\mathbf{H}_{t,F}^{M}$ created by the equivalent magnetic source (17) according to $\mathbf{H}_{t,F}^{M} = \overline{\mathbf{G}}_{EJ}^{D} \cdot \mathbf{M}_s^{eq}$ or equivalently, ($\overline{\mathbf{G}}_{EJ}^{D} \equiv \overline{\mathbf{G}}_{HM}$)

$$\mathbf{H}_{t,F}^{M} = \overline{\mathbf{G}}_{HM} \cdot \mathbf{M}_s^{eq}. \tag{26}$$

The transverse electric field created by the equivalent magnetic source (17) at the field interface $\mathbf{E}_{t,F}^{M}$ can be computed by making use of the uniqueness theorem for linear media, which ensures that all the field components inside a region without sources are determined by the tangential components of the magnetic field on the boundaries. In particular, we can determine the transverse electric field at the interface

F, $\mathbf{E}^M_{t,F}$ from the transverse magnetic field at this interface and at any other interface, provided that there are no sources between them. In this specific configuration, we will choose the interface $F-1$ as the other reference interface (although other choices are possible) and then we can write

$$\mathbf{H}^M_{t,F-1} = \overline{\mathbf{G}}^{F-1}_{HM} \cdot \mathbf{M}^{eq}_s. \tag{27}$$

Once $\mathbf{H}^M_{t,F}$ and $\mathbf{H}^M_{t,F-1}$ have been calculated, we can obtain $\mathbf{E}^M_{t,F}$ from

$$\begin{pmatrix} \mathbf{E}^M_{t,F} \\ \mathbf{H}^M_{t,F} \end{pmatrix} = \begin{pmatrix} [\mathbf{P}_{11}]_F & [\mathbf{P}_{12}]_F \\ [\mathbf{P}_{21}]_F & [\mathbf{P}_{22}]_F \end{pmatrix} \cdot \begin{pmatrix} \mathbf{E}^M_{t,F-1} \\ \mathbf{H}^M_{t,F-1} \end{pmatrix} \tag{28}$$

where the $[\mathbf{P}_{IJ}]_F$ are the (2×2) submatrices of the transition matrix, as defined in [15, Section III-A]. After straightforward manipulations, we find

$$\begin{aligned} \mathbf{E}^M_{t,F} = {} & [\mathbf{P}_{11}]_F \cdot [\mathbf{P}_{21}]^{-1}_F \cdot \mathbf{H}^M_{t,F} \\ & + ([\mathbf{P}_{12}]_F - [\mathbf{P}_{11}]_F \cdot [\mathbf{P}_{21}]^{-1}_F \cdot [\mathbf{P}_{22}]_F) \cdot \mathbf{H}^M_{t,F-1}. \end{aligned} \tag{29}$$

Now substituting in (29) the expressions given in (26) and (27), the transverse spectral magnetic Green's dyadic is finally written as

$$\begin{aligned} \overline{\mathbf{G}}_{EM} = {} & [\mathbf{P}_{11}]_F \cdot [\mathbf{P}_{21}]^{-1}_F \cdot \overline{\mathbf{G}}_{HM} \\ & + ([\mathbf{P}_{12}]_F - [\mathbf{P}_{11}]_F \cdot [\mathbf{P}_{21}]^{-1}_F \cdot [\mathbf{P}_{22}]_F) \cdot \overline{\mathbf{G}}^{F-1}_{HM} \end{aligned} \tag{30}$$

which completes the computation of the transverse electric field according to (25).

III. Numerical Examples: Radiation Characteristics of Hertzian Dipoles of Arbitrary Orientation Embedded in Complex Layered Media

Following the method described in Section II, we have developed a numerical code for computing the radiation characteristics of Hertzian electric and/or magnetic dipoles embedded in a layered bianisotropic medium. For comparison purposes, the far field was also calculated from the spectral-domain transverse electric fields in the air interface using the stationary phase technique [19, eq. 4.17(a)]. The spectral-domain transverse electric fields at the air interface were obtained following the EBM procedure described above.

First of all, we have checked our numerical results with previously published data. An initial comparison is made with the results presented in [18] and [25] for the radiation patterns of a Hertzian dipole of unit moment orientated in the x-direction and placed at the top interface of a two-layered grounded dielectric-ferrite slabs. As can be seen in Fig. 4, our data for this tangential dipole show an excellent agreement with those reported in [18] and [25]. A second example is shown in Fig. 5 for the E_θ relative far-field amplitude of an arbitrarily oriented dipole ($\varphi_{\rm dip} = 0$, $\theta_{\rm dip}$) on a grounded tilted uniaxial dielectric substrate (the optical axis orientation is set to 20°). When the dipole is placed either tangential or normal to the interfaces, our data fits properly to those shown in [13, Fig. 2].

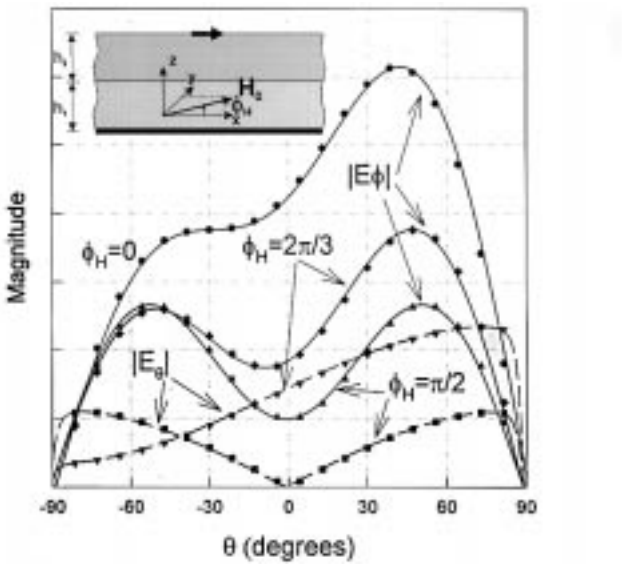

Fig. 4. Radiation pattern $|E_\theta|$ and $|E_\phi|$ versus θ in the $\phi = \pi/2$ plane for three different orientation ϕ_H ($\theta_H = \pi/2$) of the biasing magnetic field $\mathbf{H}_0$. The source is a Hertzian dipole of unit moment oriented in the x-direction and placed on top of a two-layered grounded dielectric-ferrite slabs with the following characteristics: freq: 17 GHz, $h_1 = 0.762$ mm, $h_2 = 1.524$ mm, $\epsilon_{r,1} = 12.9$, $\epsilon_{r,2} = 15.1$, $\mu_0 H_0 = 0.032$ T, $\mu_0 M_s = 0.16$ T. Solid lines: our data; symbols: data of [18] and [25].

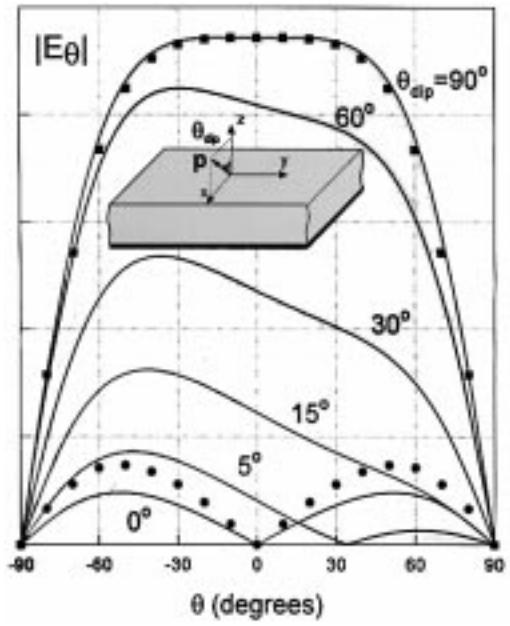

Fig. 5. E_θ far-field amplitude versus θ in the $\varphi = 0$ plane for different orientations ($\theta_{\rm dip}$) of an electric dipole $\mathbf{p}$ located at the top of a grounded uniaxial dielectric substrate with $\epsilon_{xx} = \epsilon_{yy} = 10.7\epsilon_0$, $\epsilon_{zz} = 10.4\epsilon_0$, $h = 1$ mm, and its optical axis oriented with $\theta_{\rm ax} = 20°$, $\varphi_{\rm ax} = 0°$, freq = 30 GHz. Solid lines: our data; symbols: data of [13].

In addition to these figures, and to show the possibilities of this method, we present new results for the E_θ and E_ϕ

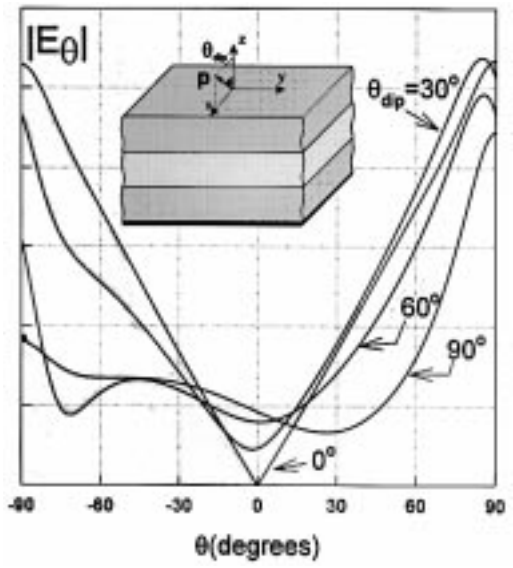

(a)

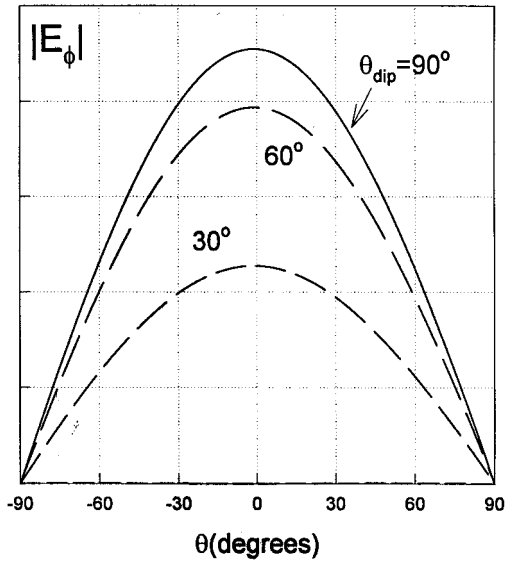

(b)

Fig. 6. Radiation pattern $|E_\theta|$ and $|E_\phi|$ versus θ in the $\phi = \pi/2$ plane for different orientation ($\theta_{\rm dip}$) of an electric dipole $\mathbf{p}$ located at the top of a three-layered grounded structure characterized by: (layer one, uniaxial dielectric) $h_1 = 1$ mm, $\epsilon_{xx} = \epsilon_{zz} = 10.7\epsilon_0$, $\epsilon_{yy} = 10.4\epsilon_0$; (layer two, magnetized ferrite) $h_2 = 1$ mm, $\epsilon_{r,2} = 15.1$, $\mu_0 M_s = 0.16$ T, $\mu_0 H_0 = 0.032$ T, $\theta_H = \pi/2$, $\varphi_H = \pi/4$; (layer three, isotropic chiral layer), $h_3 = 1$ mm, $\epsilon_{r,3} = 4$, $\mu_{r,3} = 1$, $\xi_r = -\eta_r = j0.5$.

relative far-field amplitudes of an arbitrarily oriented dipole on the top of a three-layered grounded structure comprising an uniaxial tilted dielectric, magnetized ferrite, and chiral layer. The results for several different dipole orientation are shown in Fig. 6(a) and (b). We have normalized the values of the amplitude of E_ϕ and E_θ in such a way that $(|E_\theta|_{\max})/(|E_\phi|_{\max}) = 0.11$. On the one hand, these figures show the important numerical variation of the E_ϕ far-field amplitude with respect to $\theta_{\rm dip}$ and, on the other hand, the significant qualitative changes of the E_θ relative far-field amplitude as the dipole orientation varies (especially the change of its symmetry properties).

IV. Conclusions

We have shown a systematic method for computing the CSGD for layered bianisotropic planar structures. The method makes use of the ability to express the sheets of normally directed current densities in terms of equivalent sheets of magnetic/electric-current densities parallel to the interfaces. Once the original electric sources have been entirely expressed in terms of transverse magnetic-/electric-current sheets, any of the methods used for computing the TSGD can be applied to obtain the electric and magnetic fields. In this paper, the above computation has been carried out extending the EBM to compute the corresponding transverse electric fields due to both transverse electric and magnetic surface current densities. The complete spectral electric Green's dyadic can finally be obtained after algebraically calculating the normal component of the electric field from its transverse components. For the case of magnetic currents, the complete spectral magnetic Green's dyadic can be easily obtained by applying the proper duality relations.

This method has also been applied to the computation of the far-field characteristics of arbitrarily oriented Hertzian dipoles embedded in complex layered media.

Appendix

The transverse electric spectral Green's dyadic $\overline{\mathbf{G}}_{EJ}$ in (25) is defined as the dyadic relating the transverse electric field $\mathbf{E}_{t,F}$ at the field interface F when a transverse sheet of surface electric-current density

$$\mathbf{J}_s^S = \mathbf{J}_{0,ts}\, e^{-jk_y y}\, e^{-jk_x x}\, e^{j\omega t} \tag{31}$$

is placed at the source interface S of an bianisotropic layered medium bounded by top and bottom interfaces which can be electric walls, magnetic walls, or any kind of impedance boundary conditions (IBC's). $\overline{\mathbf{G}}_{EJ}$ can be obtained from [15, eq. (5)], with (1, 2, $\cdots$) replaced by (S, F) and also considering that $\mathbf{J}_{t,F} \equiv \mathbf{J}_{t,2} = 0$ since there is not surface current at the field interface. Therefore, we have

$$0 = [\mathbf{L}]_{FS} \cdot \mathbf{E}_{t,S} + [\mathbf{L}]_{SS} \cdot \mathbf{E}_{t,F} \tag{32}$$

where $\mathbf{E}_{t,S}$ is the transverse electric field at the source interface and the $[\mathbf{L}]_{IJ}$ matrices are obtained following the recurrence algorithm given in [15, eqs. (7)–(24)], with $S \equiv 1$, $F \equiv 2$, and $K = 1, 2$. According to [15, eqs. (5) and (32)], we can write

$$\mathbf{J}_s^S = ([\mathbf{L}]_{SF} - [\mathbf{L}]_{SS} \cdot [\mathbf{L}]_{FS}^{-1} \cdot [\mathbf{L}]_{FF}) \cdot \mathbf{E}_{t,F} \tag{33}$$

which leads to the following expression for $\overline{\mathbf{G}}_{EJ}$:

$$\overline{\mathbf{G}}_{EJ} = ([\mathbf{L}]_{SF} - [\mathbf{L}]_{SS} \cdot [\mathbf{L}]_{FS}^{-1} \cdot [\mathbf{L}]_{FF})^{-1}. \tag{34}$$

As is explained in [15], the $[\mathbf{L}]_{IJ}$ matrices are expressed in terms of certain $[\mathbf{g}]_{i,j}$ and $[\mathbf{g}^{\pm}]_{i,i}$ matrices related to a single-layer problem. Explicit expressions for these matrices when both the upper and bottom interfaces are assumed to be a perfect electric wall (PEW) can be found in [15, sec. III-A, eqs. (31)–(34)]. For other types of boundary conditions, only slight changes in the $[\mathbf{g}^{\pm}]_{i,i}$ definitions corresponding to

the upper/lower interface have to be introduced. The complete expressions for the usual case of perfect magnetic wall (PMW), PEW, and any kind of interface suitable for implementation by means of IBC's are:

- PEW at the lower interface ($i = 0$)

$$[\mathbf{g}^-]_{1,1} = -[T] \cdot ([\mathbf{R}_{12}]_1^{-1} \cdot [\mathbf{R}_{11}]_1) \tag{35}$$

- PEW at the upper interface ($i = N$)

$$[\mathbf{g}^+]_{N-1,N-1} = [T] \cdot ([\mathbf{P}_{12}]_N^{-1} \cdot [\mathbf{P}_{11}]_N) \tag{36}$$

- PMW at the lower interface ($i = 0$)

$$[\mathbf{g}^-]_{1,1} = -[T] \cdot ([\mathbf{R}_{22}]_1^{-1} \cdot [\mathbf{R}_{21}]_1) \tag{37}$$

- PMW at the upper interface ($i = N$)

$$[\mathbf{g}^+]_{N-1,N-1} = [T] \cdot ([\mathbf{P}_{22}]_N^{-1} \cdot [\mathbf{P}_{21}]_N) \tag{38}$$

- IBC at the lower interface ($i = 0$) This case can be treated considering a layer below the open interface with

$$[\mathbf{g}^-]_{0,0} = -[T] \cdot [Z] \tag{39}$$

- IBC at the upper interface ($i = N$) We can now consider a layer above the $i = N$ interface with

$$[\mathbf{g}^+]_{N,N} = [T] \cdot [Z]. \tag{40}$$

For the remaining $[\mathbf{g}]_{i,j}$ matrices, the expressions in [15, eqs. (31)–(34)] still holds. The $[T]$ and $[\mathbf{R}_{ij}]$ matrices are defined in [15] and, for the usual case of free-space boundary conditions, the $[Z]$-matrix must be replaced by the well-known free-space transverse impedance matrix.

REFERENCES

[1] N. G. Alexopoulos, "Integrated-circuit structures on anisotropic substrates," *IEEE Trans. Microwave Theory Tech.*, vol. MTT-33, pp. 847–881, Oct. 1985.

[2] H. Cory, "Chiral devices—An overview of canonical problems," *J. Electromagnetic Wave Applicat.*, vol. 9, no. 5, pp. 805–829, 1995.

[3] G. T. Roome and H. A. Hair, "Thin ferrite devices for microwave integrated circuits," *IEEE Trans. Microwave Theory Tech.*, vol. MTT-16, pp. 411–420, July 1968.

[4] L. E. Davis, "Status of microwave ferrite technology in Europe," in *Proc. IEEE Microwave Theory Tech. Symp. Dig*, Atlanta, GA, 1993, pp. 199–202.

[5] D. M. Pozar, "Radiation and scattering characteristics of microstrip antennas on normally biased ferrite substrates," *IEEE Trans. Antennas Propagat.*, vol. 40, pp. 1084–1092, Sept. 1992.

[6] C. M. Krowne, "Electromagnetic properties of nonreciprocal composite chiral-ferrite media," *IEEE Trans. Microwave Theory Tech.*, vol. 41, pp. 1289–1295, Sept. 1993.

[7] I. V. Lindell, A. H. Sihvola, S. A. Tretyakov, and A. J. Viitanen, *Electromagnetic Waves in Chiral and Bi-isotropic Media.* Norwood, MA: Artech House, 1994.

[8] C. T. Tai, *Dyadic Green's Functions in Electromagnetic Theory.* New York: International Publishers, 1971.

[9] P. H. Pathak, "On the eigenfunction expansion of electromagnetic dyadic Green's functions," *IEEE Trans. Antennas Propagat.*, vol. AP-31, pp. 837–846, Nov. 1983.

[10] W. C. Chew, *Waves and Fields in Inhomogeneous Media.* New York: Van Nostrand, 1990.

[11] G. Dural and M. I. Aksun, "Closed-form Green's functions for general sources and stratified media," *IEEE Trans. Microwave Theory Tech.*, vol. 43, pp. 1545–1552, July 1995.

[12] C. M. Krowne, "Fourier transformed matrix method of finding propagation characteristics of complex anisotropic layered media," *IEEE Trans. Microwave Theory Tech.*, vol. MTT-32, pp. 1617–1625, Dec. 1984.

[13] J. L. Tsalamengas and N. K. Uzunoglu, "Radiation from a dipole in the proximity of a general anisotropic grounded layer," *IEEE Trans. Antennas Propagat.*, vol. AP-33, pp. 165–172, Feb. 1985.

[14] R. Marqués and M. Horno, "On the spectral dyadic Green's function for stratified linear media. Application to multilayered MIC lines with anisotropic substrates," *Proc. Inst. Elect. Eng.* vol. 134, pt. H, pp. 241–248, June 1987.

[15] F. Mesa, R. Marqués, and M. Horno, "A general algorithm for computing the bidimensional spectral dyadic Green's function: The equivalent boundary method (EBM)," *IEEE Trans. Microwave Theory Tech.*, vol. 39, pp. 1640–1649, Sept. 1991.

[16] J. T. Aberle and D. M. Pozar, "Analysis of infinite arrays of probe-feed rectangular microstrip patches using a rigorous feed model," *Proc. Inst. Elect. Eng.* vol. 136, pt. H, pp. 110–119, Apr. 1989.

[17] R. E. Collin, *Field Theory of Guided Waves*,2nd ed. Piscataway, NJ: IEEE Press, 1991.

[18] R. R. Boix, N. G. Alexopoulos, and M. Horno, "Efficient numerical computation of the spectral transverse dyadic Green's function in stratified media," *J. Electromagn. Waves Applicat.*, vol. 10, pp. 1045–1081, 1996.

[19] R. E. Collin, *Antennas and Radiowave Propagation.* New York: McGraw-Hill, 1985.

[20] L. Vegni, R. Cicchetti, and P. Capece, "Spectral dyadic Green's function formulation for planar integrated structures," *IEEE Trans. Antennas Propagat.*, vol. 36, pp. 1057–1065, Aug. 1988.

[21] J. L. Tsalamengas, "Electromagnetic fields of elementary dipole antennas embedded in stratified general gyrotropic media," *IEEE Trans. Antennas Propagat.*, vol. 37, pp. 399–403, Mar. 1989.

[22] R. F. Harrington, *Time-Harmonic Electromagnetic Fields.* New York: McGraw-Hill, 1961.

[23] J. L. Tsalamengas, "Interaction of electromagnetics waves with general bianisotropic slabs," *IEEE Trans. Microwave Theory Tech.*, vol. 40, pp. 1870–1878, Oct. 1992.

[24] G. Plaza, F. Mesa, and M. Horno, "Computation of propagation characteristics of chiral layered waveguides," *IEEE Trans. Microwave Theory Tech.*, vol. 45, pp. 519–526, Apr. 1997.

[25] I. Y. Hsia and N. G. Alexopoulos, "Radiation characteristics of Hertzian dipole antennas in a nonreciprocal superstrate–substrate structure," *IEEE Trans. Antennas Propagat.*, vol. 40, pp. 782–790, July 1992.

Francisco Mesa (M'94), for photograph and biography, see this issue, p. 1071.

Ricardo Marqués (M'95) was born in San Fernando, Cádiz, Spain. He received the Licenciado and Doctor degrees from the University of Seville, Seville, Spain, in 1983 and 1987, respectively, both in physics.

Since January 1984, he has been with the Department of Electronics and Electromagnetism, University of Seville, where he is currently an Associate Professor. His main field of interest includes microwave integrated circuit (MIC) devices, wave propagation in complex and anisotropic media, and field theory.

Manuel Horno (M'75), for photograph and biography, see this issue, p. 1157.